Structure of the quasi-one-dimensional Si(553)-Au surface: Gold dimer row and silicon honeycomb chain

Wolfgang Voegeli,* Toru Takayama, Tetsuroh Shirasawa, Makoto Abe, Kimitaka Kubo, and Toshio Takahashi
Institute for Solid State Physics, University of Tokyo, 5-1-5 Kashiwanoha, Kashiwa 277-8581, Japan

Koichi Akimoto
Department of Quantum Engineering, Nagoya University, Furo-cho, Chikusa-ku, Nagoya 464-8603, Japan

Hiroshi Sugiyama
Photon Factory, High Energy Accelerator Research Organization, Tsukuba 305-0801, Japan
(Received 30 April 2010; published 26 August 2010)

The Si(553)-Au surface consists of a periodic array of single steps and (111) terraces with a quasi-one-dimensional electronic structure. In this paper, the determination of the atomic structure of this surface with x-ray diffraction is reported. The gold coverage of the surface was measured to be 0.5 monolayer using x-ray fluorescence spectroscopy, i.e., two gold atoms per primitive unit cell. A structural model was constructed directly from the x-ray diffraction intensities with a step-by-step approach. First, the relative positions of the gold atoms were obtained from the Patterson map. Using the positions of the gold atoms, the deconvolution of the Patterson map was calculated and the positions of the gold atoms relative to the substrate were determined. Finally, the positions of the silicon atoms at the surface were obtained from a reconstruction of the electron density with an iterative phase and amplitude recovery algorithm. The main features of the structural model obtained in this way are a row of gold dimers on the (111) terraces in the topmost layer of the surface, and a honeycomb chain of silicon atoms near the step edge. Structural refinement of this model with the experimental diffraction data gave reasonable atomic positions and a χ^2 value of 3.35, better than previous models. The model is related to the $\times 2$ m1 model recently proposed by Krawiec [Phys. Rev. B **81**, 115436 (2010)] but without the strong $\times 2$ modulation.

DOI: 10.1103/PhysRevB.82.075426 PACS number(s): 68.35.bg, 68.47.Fg, 61.05.cp

I. INTRODUCTION

Deposition of submonolayer amounts of metal atoms onto silicon surfaces can lead to the formation of anisotropic surface structures with electronic states that are highly confined into one dimension. These structures have been investigated with a view to how their nearly one-dimensional atomic and electronic structures influence the physical properties. For example, in many cases metal-insulator transitions or other phase transitions occur on these surfaces. As prominent examples the Si(111)-4×1-In and the Si(111)-5×2-Au surfaces have been studied for a long time, but there are still many unresolved questions, even on such basic issues as the atomic structure. Since about 10 years ago, one-dimensional structures on vicinal surfaces of silicon have attracted interest.[1] These surfaces consist of periodic arrays of steps separated by terraces with a (111) orientation. The presence of the steps naturally leads to the formation of highly anisotropic structures. The electronic structure and the strength of the two-dimensional coupling can be varied depending on the vicinal angle of the surface and the type of adsorbate atoms.

The Si(553)-Au surface obtained by depositing submonolayer amounts of gold onto the Si(553) surface is an example for such a structure.[2] It is composed of 1.5-nm-wide terraces with a (111) orientation, separated by single bilayer steps. The electronic structure is metallic with a highly one-dimensional character along the steps.[2] An interesting feature is that two metal-insulator transitions occur on the surface, in which two different local superstructures appear in different parts of the unit cell.[3,4] In addition, the electronic structure is significantly influenced by the Rashba effect.[5] This surface can be prepared with a high quality and could also be used as a template for the further growth of one-dimensional structures, as has been done for Pb on the Si(335)-Au surface[6] and In on the Si(553)-Au surface,[7] or as a template for the adsorption of organic molecules.

The structure of the Si(553)-Au surface has been investigated theoretically and experimentally by several groups[2,8–13] but without reaching a consensus. A problem is that the gold coverage is still under discussion. Until recently, most authors assumed a gold coverage of 0.25 monolayer (ML), i.e., one gold atom per primitive unit cell. Recently, however, evidence has been presented that the gold coverage is 0.5 ML, i.e., two gold atoms per primitive unit cell.[14] An early model with a gold double row at the step edge proposed by Ghose *et al.*[8] from x-ray diffraction was later shown to be unstable in *ab initio* calculations.[9] Other proposed models have a single row of gold atoms substituting for silicon in the top-most surface layer.[2,10–13] Very recently, Krawiec[15] has investigated several models with two gold atoms theoretically, and found two models that reproduce the experimental band structure and scanning tunneling microscopy (STM) images reasonably well. The $\times 1$ m1 model has a 1×1 structure, like the high temperature Si(553)-Au surface. When a $\times 2$ superstructure parallel to the steps was allowed, the model changed significantly to the $\times 2$ m1 model.

We have determined the structure of the Si(553)-Au surface from surface x-ray diffraction and obtained a model with two gold atoms per primitive unit cell directly from the experimental intensities. The gold atoms arrange in a double row parallel to the steps as in the model of Ghose *et al.*, but on the terraces. The Si atoms near the step edge form a honeycomb chain. The model is closely related to the $\times 2$ m1 model, although it was determined without knowledge of Ref. 15. It does not have the $\times 2$ modulation of the $\times 2$ m1 model, however, and it is incompatible with the $\times 1$ m1 model suggested as the high-temperature phase in Ref. 15.

II. EXPERIMENTAL METHODS

The x-ray diffraction experiments were done with the ultrahigh vacuum surface diffractometer at beamline 15B2 of the Photon Factory at KEK.[16] The sample was a P-doped Si(553) wafer ($\rho=2-4\ \Omega$ cm). The experiments were done in ultrahigh vacuum (base pressure 1×10^{-8} Pa).

The sample preparation was similar to our previous reports.[13,17,18] First a clean Si(553) surface was prepared by flashing the sample to 1250 °C. Then gold was deposited onto the sample at 600 °C, followed by annealing at 850 °C for 5 s. The vacuum was about 2×10^{-7} Pa during the deposition. A sharp specular spot in the reflection high-energy electron diffraction (RHEED) pattern confirmed that the surface structure was of high quality.

A centered orthorhombic surface unit cell with two steps per unit cell is used in this paper.[8] The real space coordinates x, y, and z are in the $[3\bar{3}10]$ (perpendicular to the steps), $[1\bar{1}0]$ (parallel to the steps), and [553] (perpendicular to the surface) directions. h, k, and l are the corresponding Miller indices of reciprocal space. The size of the unit cell is 29.5 Å in the x direction, 3.84 Å in the y direction, and 41.7 Å in the z direction.

X-ray diffraction measurements were done at room temperature with a wavelength of 1.07 Å. Intensities of 54 crystal truncation rods (CTRs) with $l=1.5-14.8$ were collected. The integrated intensities were corrected for the scattering geometry, polarization and active sample area.[19] Averaging of symmetry-equivalent intensities resulted in 34 symmetry-independent CTRs with 616 data points. CTRs with $k=0$ could not be measured due to constraints of the sample holder. The systematic error of the intensities estimated from the symmetry-related data points was 16%.[20] The experimental data are available in the online supplementary materials.[21]

The Si(553)-Au surface undergoes a phase transition slightly above room temperature, in which a $\times 2$ superstructure forms in the direction of the steps.[3,4] Half-order streaks from this superstructure were visible both with RHEED and x-ray diffraction but x-ray intensities could only be measured for a few half-order reflections because of the low intensity. It was difficult to find a common scale of the integrated intensities of the half-order reflections and the CTRs because the former are streaks in reciprocal space while the latter are sharp spots. The half-order reflections were not included in the analysis for this reason.

The gold coverage was determined *ex situ* with x-ray fluorescence spectroscopy at beam line 15B1 of the Photon Factory. The exciting x-rays had an energy of 12.78 keV. The intensity of the Au $L\alpha$ fluorescence line was measured with a CdTe detector (Amptek XR-100T) in the polarization plane of the incident x-rays at an angle of about 85° with respect to the incident direction.

III. RESULTS

A. Gold coverage

A fundamental piece of information necessary in order to determine a surface structure is the coverage of adsorbate atoms. For the Si(553)-Au surface, most authors have assumed an Au coverage of 0.25 ML (one Au atom per unit cell) (e.g., Refs. 2 and 11–13). A recent measurement of the gold coverages of the Si(557)-Au, Si(111)-5×2-Au, and Si(553)-Au surfaces by Barke *et al.*,[14] however, has found a gold coverage of 0.5 ML for the Si(553)-Au surface, i.e., two Au atoms per unit cell, in agreement with the x-ray diffraction investigation by Ghose *et al.*[8]

We have measured the relative gold coverages of the Si(557)-Au, Si(111)-5×2-Au, and Si(553)-Au surfaces using x-ray fluorescence spectroscopy. The gold coverages were determined by comparing the intensities of the Au $L\alpha$ fluorescence peak of the three surfaces. The ratio of the peak intensity of the Si(557)-Au surface to that of the Si(553)-Au surface was 2.48 and the ratio of the intensity of the Si(557)-Au surface to that of the Si(111)-5×2-Au surface was 2.96. Assuming a gold coverage of 0.2 ML for the Si(557)-Au surface[2,22,23] gives coverages of 0.50 ML for the Si(553)-Au surface and 0.59 ML for the Si(111)-5×2-Au surface.

These coverages are in good agreement with those found by Barke *et al.*[14] The correctness of the results depends on the correctness of the gold coverage of 0.2 ML for the Si(557)-Au surface. This coverage corresponds to one gold atom per unit cell. A coverage of two gold atoms for the Si(557)-Au surface would lead to twice as large gold coverages for the Si(553)-Au and Si(111)-5×2-Au surfaces, which is much larger than other estimations. In addition, coverages of one gold atom for the Si(557)-Au surface and two gold atoms for the Si(553)-Au surface explain the x-ray diffraction data well (see the next section and Refs. 8 and 24).

B. Model construction

To solve a complex structure like the Si(553)-Au surface, it is necessary to obtain as much information as possible directly from the experimental diffraction intensities. We adopted a step-by-step approach, in which first the positions of the heavy gold atoms were determined, then the positions of the surface Si atoms.

The simplest way to obtain information directly from the diffraction intensities is by Fourier transforming the intensities. This gives the autocorrelation function of the electron density, the Patterson map[25]

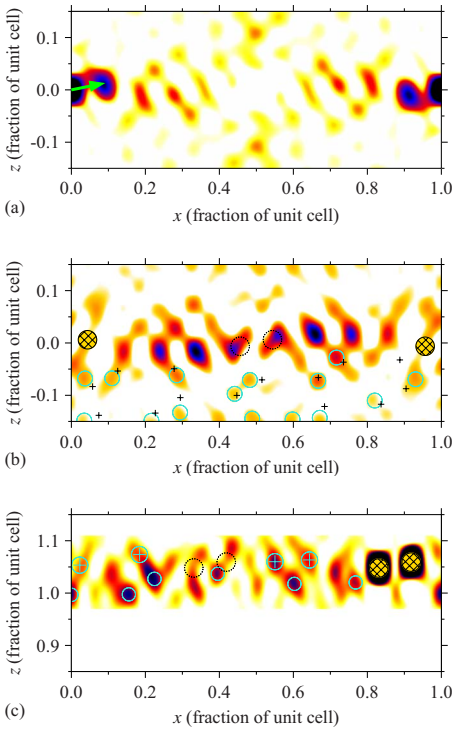

FIG. 1. (Color online) (a) Patterson map of the Si(553)-Au surface. The arrow indicates the interatomic vector of the two gold atoms. (b) Patterson map deconvolved with the electron density of the two gold atoms [Eq. (8)]. The contribution of the gold atoms was subtracted. (c) Reconstructed electron density. Hashed yellow circles in (b) and (c) mark the positions of the two gold atoms, dashed black circles the positions of gold atoms at $y=0.5$. Blue circles show the positions of atoms determined from the maps, the blue circles with a cross the positions of atoms in the honeycomb chain. The black crosses in (b) indicate the ideal positions of bulk Si atoms. For all three maps, x is in the surface plane perpendicular to the steps and z perpendicular to the surface. The maps show a section at $y=0.0$, the section at 0.5 can be obtained by shifting x by 0.5. Negative values were set to zero.

$$P(x,y,z) = \frac{1}{V}\sum_{hkl} |F_{hkl}|^2 \cos[2\pi(hx+ky+lz)], \tag{1}$$

where F_{hkl} is the structure factor of the reflection with Miller indices (h,k,l), and V the volume of the unit cell. Peaks in $P(x,y,z)$ correspond to interatomic vectors between two atoms. The intensity of the peaks is proportional to the product of the electron densities of the two atoms.

Figure 1(a) shows a section of the Patterson map at $y=0$. The strongest peak in the Patterson map besides the origin is at about $x=0.088$, $z=0.013$ (The peak at $x=0.912$, $z=-0.013$ is its inversion image). This peak can be interpreted as the interatomic vector between the two gold atoms in the unit cell as indicated by the arrow in Fig. 1(a) because gold has a much higher electron density than silicon. The gold-gold distance is about 2.64 Å.

The other peaks in the Patterson map correspond to vectors between Si atoms and Au atoms. Si-Si vectors are too weak to be visible. Extracting the positions of the Si atoms from the Patterson map is difficult because there are many peaks from Si-Au interatomic vectors, which partly overlap. In addition, test calculations of Patterson maps for model structures showed that the Patterson map is distorted by Fourier ripples of the gold peaks caused by the truncation of the Fourier series. Near the Au peaks, the ripples can be comparable in peak height to the Si-Au peaks because the gold atoms are much heavier than the Si atoms. Some real Si-Au peaks are shifted by this effect, or are reduced in intensity. We therefore used methods that are easier to interpret for the further structure determination, as explained in the following.

An approximate deconvolution of the Patterson map was performed to obtain information about the positions of the gold atoms relative to the substrate. The Patterson map can be seen as the convolution of the electron density $\rho(\vec{r})$ with its inversion image

$$P(\vec{r}) = \rho(-\vec{r}) \otimes \rho(\vec{r}), \tag{2}$$

where $\otimes$ denotes convolution. The electron density is the sum of the electron density of the gold atoms and the silicon atoms

$$\rho(\vec{r}) = \rho_{\mathrm{Au}}(\vec{r}) + \rho_{\mathrm{Si}}(\vec{r}). \tag{3}$$

Inserting Eq. (2) into Eq. (3) gives

$$\begin{aligned} P(\vec{r}) &= \rho_{\mathrm{Au}}(-\vec{r}) \otimes \rho_{\mathrm{Au}}(\vec{r}) + \rho_{\mathrm{Au}}(-\vec{r}) \otimes \rho_{\mathrm{Si}}(\vec{r}) \\ &\quad + \rho_{\mathrm{Si}}(-\vec{r}) \otimes \rho_{\mathrm{Au}}(\vec{r}) + \rho_{\mathrm{Si}}(-\vec{r}) \otimes \rho_{\mathrm{Si}}(\vec{r}), \end{aligned} \tag{4}$$

$$\approx \rho_{\mathrm{Au}}(\vec{r}) \otimes [\rho_{\mathrm{Au}}(\vec{r}) + \rho_{\mathrm{Si}}(\vec{r}) + \rho_{\mathrm{Si}}(-\vec{r})]. \tag{5}$$

The term $\rho_{\mathrm{Si}}(-\vec{r}) \otimes \rho_{\mathrm{Si}}(\vec{r})$ has been neglected in Eq. (5) because the electron density of the gold atoms is much larger than that of the silicon atoms. In addition, for two gold atoms ρ_{Au} is centrosymmetric if the origin of the coordinate system is chosen at the center of the two gold atoms, so $\rho_{\mathrm{Au}}(-\vec{r}) = \rho_{\mathrm{Au}}(\vec{r})$. Since ρ_{Au} is determined by the relative positions of the gold atoms, which are known from the Patterson map, Eq. (5) can be deconvolved by Fourier transforming it

$$\mathcal{F}[P(\vec{r})] = \mathcal{F}[\rho_{\mathrm{Au}}(\vec{r})]\mathcal{F}[\rho_{\mathrm{Au}}(\vec{r}) + \rho_{\mathrm{Si}}(\vec{r}) + \rho_{\mathrm{Si}}(-\vec{r})]. \tag{6}$$

The Fourier transform of P is proportional to the experimental intensities $\mathcal{F}(P) = |F|^2 = cI_{exp}$ with a scale factor c, and the Fourier transform of ρ_{Au} is the structure factor of the two gold atoms F_{Au}. One can therefore rewrite Eq. (6) in the following way:

$$cI_{exp} = F_{\mathrm{Au}}\{F_{\mathrm{Au}} + \mathcal{F}[\rho_{\mathrm{Si}}(\vec{r}) + \rho_{\mathrm{Si}}(-\vec{r})]\} \tag{7}$$

and Fourier transform it to obtain an approximation of the electron density of the silicon atoms superimposed with its inversion image

$$\rho_{\mathrm{Si}}(\vec{r}) + \rho_{\mathrm{Si}}(-\vec{r}) = \mathcal{F}\left(\frac{cI_{exp}}{F_{\mathrm{Au}}}\right) - \mathcal{F}(F_{\mathrm{Au}}). \tag{8}$$

A problem in the application of Eq. (8) is that the scale factor c is usually not known, because the absolute value of the experimental intensities I_{exp} is difficult to measure. It can be estimated if the numbers and types of scattering atoms are

known. This is usually the case in the determination of bulk structures, but for a surface structure the number of atoms contributing is generally difficult to estimate. Fortunately, in the present case, the number of gold atoms is known. This allows us to estimate the scale factor by comparing the intensities of the peaks from the gold atoms in the Patterson map to the origin peak. The intensities of the peaks are proportional to the sum of the squared number of electrons of the contributing atoms, the gold atoms in the case of the gold peak, and all atoms in the case of the origin peak. The ratio of the two peaks gives the ratio of the scale factor calculated for two gold atoms to the real scale factor. Strictly speaking, the volume of the peaks has to be used, but we found that using the peak height gave adequate results. The deconvolved Patterson map did not change dramatically when the scale factor was changed 10–20 %.

We found that in the calculation of the structure factor of the gold atoms, F_{Au}, the Debye-Waller temperature factor of the gold atoms has to be taken into account. The Debye-Waller factor was estimated from the Wilson plot[26] to 10.5 $\mathrm{\AA}^2$, that is, a mean square amplitude of atomic vibrations $\overline{u^2}$ of 0.13 $\mathrm{\AA}^2$.

Equation (8) is applicable when the scattering from the gold atoms is the largest contribution to the total intensity. This is generally not true at each point in reciprocal space, even if it is true on average. For example, the contribution from the bulk atoms is much larger than from the surface atoms near Bragg peaks. In addition, in the case of the present surface structure, there are points in reciprocal space for which the scattering amplitudes from the two gold atoms are out-of-phase and therefore cancel. When Eq. (8) is applied, the Fourier components corresponding to these regions in reciprocal space will be large, since $cI_{exp} \gg F_{\mathrm{Au}}$, but their phase is likely not correct. It is better to neglect these Fourier components. In the present work only Fourier components with $F_{\mathrm{Au}} > \frac{1}{2} cI_{exp}$ were used.

The deconvolution of the Patterson map using Eq. (8) is shown in Fig. 1(b). The strong peaks near $z=0$ are due to the silicon atoms at the surface or their inversion images. Peaks at larger negative z are due to substrate atoms, those at larger positive z are their inversion images. The deconvolution of the Patterson map is distorted by the Fourier ripples of the gold atoms, as in the case of the Patterson map. Nevertheless, inspection of the peaks at negative z shows that most of them can be identified with bulklike Si atoms. These peaks are indicated with blue circles in Fig. 1(b). The positions of the gold atoms relative to the substrate can be inferred from their positions. The black crosses indicate the ideal positions of the bulk atoms.

Peaks of the surface Si atoms are clearer in the deconvolution of the Patterson map than in the Patterson map. However, there still is the ambiguity that the map contains both the electron density of the silicon atoms and its inversion image. An approximation of the electron density without this ambiguity can be obtained using the known positions of the gold atoms and the substrate silicon atoms. The scattering is dominated by the substrate near the Bragg peaks and by the gold atoms almost everywhere else. The real structure factors are therefore close to those calculated for a model containing only the substrate atoms and the gold atoms. The positions of the other atoms can then be determined by difference Fourier synthesis,[20] a holographic method,[27] or iterative phase recovery methods. Application of each of the three methods leads to similar surface models. In the following the results of the application of the *phase and amplitude recovery and diffraction image generation method* (PARADIGM) algorithm of Saldin *et al.*[28–30] to obtain the electron density of the silicon atoms are presented. This algorithm recovers the electron density directly from the measured structure factors by iteratively applying constraints in real space and reciprocal space. The surface electron density is constrained in real space to be positive and to vanish above and below the surface region. The surface region was chosen to be from 3.3 Å below to 2.6 Å above the left gold atom. In reciprocal space, the agreement with the measured structure factors is enforced.

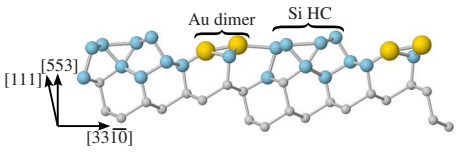

FIG. 2. (Color online) Side view of the model constructed from the electron density map. Large yellow spheres are gold atoms, blue spheres are Si atoms obtained from the electron density map, and small gray spheres are bulk Si atoms. The surface consists of a gold dimer row and a Si honeycomb chain.

The algorithm was started with the surface electron density of the gold atoms in the positions relative to the bulk determined from the deconvolution of the Patterson map. The phases of the structure factors calculated from this electron density are already close to the real ones, and the algorithm converged in a few iterations. The reconstructed electron density is shown in Fig. 1(c). The positions of the surface atoms can be determined from the peaks of the density map. Figure 2 shows the structural model obtained in this way. The empty blue circles in Fig. 1(c) mark the peaks with positions close to those expected from a continuation of the bulk. Si atoms placed at the positions of the peaks marked with the blue circles with a cross inside form a so-called honeycomb chain,[31] a common feature in surface structures induced by gold on silicon.[24,32] The atoms in the honeycomb chain have a nearly planar threefold bonding configuration, similar to graphene.

Test calculations showed that the reconstructed density in the vicinity of the gold atoms is distorted by Fourier ripples, as in the case of the Patterson map, so peaks in that region are not reliable. The honeycomb chain and most of the bulklike atoms are clearly resolved in the electron density map but the Si atoms immediately left [$x,z=0.77,1.02$ in Fig. 1(c)], right (0.02,1.05) and especially between (0.40, 1.04) the gold atoms are influenced by the Fourier ripples. The presence of these atoms makes sense considering the bonding configuration but their exact position has to be determined from the structural refinement below. No atoms were placed on the peaks at (0.11,1.03), at (0.71,1.04) and near the gold atoms, because that would lead to unreasonable bonding configurations. These peaks are probably caused by the Fourier ripples or by holes in the experimental data.

C. Structural refinement

The atomic positions in the model in Fig. 2 were refined by least-squares fitting to the experimental intensities. Variations in the model and previously proposed models were fitted as well, to check whether other models give a better fit. Positions of the atoms in the top-most layer and their isotropic Debye-Waller factors were used as parameters. The fitting was repeated about 1000 times with different starting parameters to ensure that a global minimum for each model was found. The quality of the fit was judged using the χ^2 value.

Fitting of the model in Fig. 2 gave a χ^2 value of 3.6. The atomic positions in the fitted structure were very similar to the starting model. Some variations in the model in Fig. 2 were investigated as well. First, the presence of the Si atom between the two gold atoms was checked. The electron density map is distorted by the close proximity to the gold atoms in this region and the presence or absence of this Si atom is difficult to judge from the electron density map. A model without this atom gave a significantly higher χ^2 value of 6.3. It was also tried to place additional adatoms above the gold atoms, above the honeycomb chain and as an extension of the step edge. These models gave lower values of χ^2 but the adatom moved to unphysical positions in all cases. It was therefore concluded that no adatom is present, in agreement with STM images.[11]

Previously proposed models were fitted as well. The model by Ghose *et al.* gave a best-fit χ^2 value of 4.3. The refined model was completely changed from the starting model and the Si atoms had unphysical bonding configurations. Riikonen *et al.* have studied a number of models with a gold coverage of 0.25 ML with density functional calculations.[12] The models with the lowest energy in that paper are called the f2, f3, and f4 models. They consist of a Si honeycomb chain at the step edge and a gold atom in different positions on the terrace. Riikonen *et al.* favor the f2 model based on the comparison of the electronic structure to experiment while a density-functional theory and STM study by Ryang *et al.*[11] favored the f4 model based on the similarity of the STM images to experimental ones. The f3 model gave the best agreement of experimental and calculated Patterson maps in a previous x-ray diffraction study by us.[13] Fitting of these models gave χ^2 values of 5.3, 6.6, and 6.3 for the f2, f3, and f4 models, respectively. They can therefore be excluded.

The weak half-order streaks observed both with RHEED and x-ray diffraction indicate that the sample has a weak 1×2 structure. The influence of the 1×2 structure on the intensities is too small for a complete determination of the nature of the $\times2$ superstructure including the Si atoms. For this, measurements at low temperature have to be done. We have, however, tried to fit a $\times2$ superstructure of the gold atoms, in which the gold atoms were allowed to move parallel to the steps. If the two gold atoms move in opposite directions parallel to the steps, then the model in Fig. 2 is similar to the $\times2$ m1 model of Krawiec.[15] Only the integer-order intensities were used in the fit but a $\times2$ superstructure can be detected by split positions of the atoms. Several configurations with almost the same χ^2 were found. The left gold atom moved by between 0.13 Å and 0.03 Å parallel to the steps but the right gold atom stayed at the symmetric position. The χ^2 value did not change with regard to the $\times1$ structure, hence it is not possible to judge whether the gold atoms form a $\times2$ structure. Any possible displacement along the steps is smaller than in the $\times2$ m1 model, however, where the gold atoms are both displaced by about 0.26 Å from the symmetric positions of Fig. 2.[33]

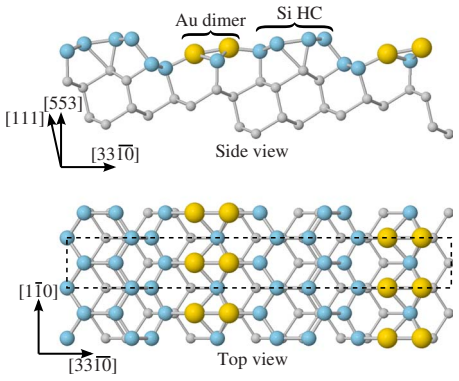

FIG. 3. (Color online) Structural model after the refinement of the atomic positions. Large yellow spheres are gold atoms, blue spheres Si atoms in the top-most layer, and small gray spheres bulk Si atoms. The dashed rectangle indicates the centered surface unit cell.

Finally, the least-square fit of the model in Fig. 2 was repeated including some substrate Si atoms in the second bilayer. This reduced χ^2 slightly to 3.35 but did not change the model significantly. The refined model is shown in Fig. 3. The refined atomic coordinates are available in the online supplementary materials.[21] Examples of the agreement between the calculated CTR profiles and the experimental data are shown in Fig. 4.

IV. DISCUSSION

Krawiec[15] found in their *ab initio* calculations two models that gave reasonable agreement with the experimental band structures, the $\times1$ m1 and $\times2$ m1 models. They were tentatively assigned as the high-temperature and low-temperature phases, respectively. The $\times2$ m1 model developed from the $\times1$ m1 model when a $\times2$ superstructure along the steps was allowed but it has a fundamentally different bonding configuration. The $\times1$ m1 model is incompatible with the Patterson map in Fig. 1(a) because it would have a very different position of the Au-Au peak. The $\times2$ m1 model, however, is in fact closer to the model in Fig. 3 than to the $\times1$ m1 model from which it was derived. The $\times2$ m1 model could therefore be the low temperature structure of the present model. It should be pointed out, however, that there is a fundamental difference in the band structure of the $\times2$ m1 model compared to experiment at low temperatures:[3,4] the former is metallic, while in the latter a band gap opens when the $\times2$ superstructure forms. The metallic surface is also in conflict with the experimental classification of the transition as a Peierls transition.[3,4,17] The formation of the low-temperature phase needs therefore further investigation.

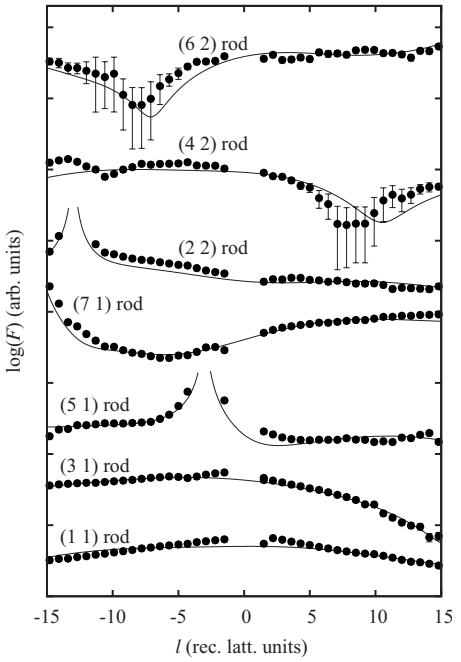

FIG. 4. Comparison of measured structure factors F (solid circles) and those calculated from the best-fit model (lines) for representative CTRs. The curves are vertically offset for clarity.

The model for the Si(553)-Au surface has similarities with models for other gold chain structures on silicon surfaces, the Si(557)-Au, Si(335)-Au, and Si(111)-5×2-Au surfaces. The silicon honeycomb chain is a common structural component in metal-induced surface structures on the Si(111) surface and vicinal surfaces.[31] In the case of models for the Si(557)-Au and Si(335)-Au surfaces, the honeycomb chain is located at the step edge[24,34] as in the present model. Models for the Si(111)-5×2-Au surface proposed from *ab initio* calculations also have a honeycomb chain next to a double gold row.[32,35] The local structure of the gold double row is similar to the one in the present model. There is no experimental confirmation of the models for the Si(111)-5×2-Au and Si(335)-Au surface yet, so the present structure can be seen as giving support to these models as well.

An interesting question is why the gold atoms form a double row on this surface, in contrast to the single rows on the closely related Si(557)-Au and Si(335)-Au surfaces. The Si(557)-Au surface has wider terraces than the Si(553)-Au surface (19.1 Å compared to 14.7 Å) so naively one could expect that more gold atoms would fit onto the terraces of the Si(557)-Au surface. There are two possible explanations. The first is the instability of Si dangling bonds, an important driving force for reconstructions on Si surfaces.[36] If the Si(553)-Au surface would be composed of a honeycomb chain and a single gold row, for example, by replacing one of the gold atoms with silicon in Fig. 3, then a Si dangling bond would be created on the terraces, which cannot be saturated easily. In the case of the Si(557)-Au and Si(335) surfaces, on the other hand, either no Si dangling bonds (except for the step edge atoms) are present, or the dangling bonds are saturated by adatoms.[24,34] If there were two gold rows on the Si(557)-Au surface, then the saturation by the adatoms would not be possible and a row of dangling bonds would be created. Another possible reason might be that the honeycomb chain necessarily introduces a stacking fault, which has to be corrected for by a surface dislocation on the terrace.[10] At the dislocation a silicon atom bonded to four neighbors in the surface plane appears. This atom is situated between the gold atoms in the present model. It is easily imaginable that this bonding configuration is only stable if the four neighbors are all gold atoms. The honeycomb chain on the Si(557)-Au and Si(335) surfaces does not create a stacking fault so similar bonding configurations do not appear.

The structure of the gold double row is also interesting. The two gold rows are separated by 2.67 Å, somewhat smaller than the interatomic distance in gold of 2.88 Å. The atomic distances in the same row are 3.84 Å. The gold double row can therefore be seen as a row of gold dimers. The connection in the direction of the steps is provided via Si atoms.

V. CONCLUSION

The atomic structure of the Si(553)-Au surface was determined with surface x-ray diffraction. The gold coverage was found to be 0.5 ML, in agreement with a previous x-ray investigation[8] and a recent determination of the gold coverage.[14] A combination of different methods for directly obtaining structural information from the diffraction intensities proved to be effective for the structure determination.

The structure consists of a row of gold dimers on the (111) terraces and a Si honeycomb chain near the step edges. It is closely related to the ×2 m1 model of Krawiec, which might be the low temperature structure of the surface.[15] The determination of the structure should help to clarify the origin of the metallic band structure and the two metal-insulator phase transitions.

ACKNOWLEDGMENTS

The present work was partly supported by Grant-in-Aids for Scientific Research (Grants No. 19-07093 and No. 22-360018) from the Ministry of Education, Culture, Sports, Science and Technology, Japan, and by the Hori Information Science Promotion Foundation. The synchrotron radiation experiments were done at beamlines 15B2 and 15B1 of the Photon Factory under the approval of the Photon Factory Program Advisory Committee (Proposals No. 2006S2-003, No. 2008G083, No. 2008G152, and No. 2009G612). W.V. thanks the Japan Society for the Promotion of Science (JSPS).

*Corresponding author; wvoegeli@issp.u-tokyo.ac.jp

[1] For recent reviews, see, e.g., P. C. Snijders and H. H. Weitering, Rev. Mod. Phys. **82**, 307 (2010); I. Barke, R. Bennewitz, J. N. Crain, S. C. Erwin, A. Kirakosian, J. L. McChesney, and F. J. Himpsel, Solid State Commun. **142**, 617 (2007).

[2] J. Crain, A. Kirakosian, K. Altmann, C. Bromberger, S. Erwin, J. McChesney, J. Lin, and F. Himpsel, Phys. Rev. Lett. **90**, 176805 (2003).

[3] J. Ahn, P. Kang, K. Ryang, and H. Yeom, Phys. Rev. Lett. **95**, 196402 (2005).

[4] P. Snijders, S. Rogge, and H. Weitering, Phys. Rev. Lett. **96**, 076801 (2006).

[5] I. Barke, F. Zheng, T. K. Rugheimer, and F. J. Himpsel, Phys. Rev. Lett. **97**, 226405 (2006).

[6] M. Kisiel, K. Skrobas, R. Zdyb, P. Mazurek, and M. Jalochowski, Phys. Lett. A **364**, 152 (2007).

[7] P.-G. Kang, H. Jeong, and H. W. Yeom, Phys. Rev. B **79**, 113403 (2009).

[8] S. Ghose, I. Robinson, P. Bennett, and F. Himpsel, Surf. Sci. **581**, 199 (2005).

[9] S. Riikonen and D. Sánchez-Portal, Surf. Sci. **600**, 1201 (2006).

[10] S. Riikonen and D. Sánchez-Portal, Nanotechnology **16**, S218 (2005).

[11] K.-D. Ryang, P. G. Kang, H. W. Yeom, and S. Jeong, Phys. Rev. B **76**, 205325 (2007).

[12] S. Riikonen and D. Sánchez-Portal, Phys. Rev. B **77**, 165418 (2008).

[13] T. Takayama, W. Voegeli, T. Shirasawa, K. Kubo, M. Abe, T. Takahashi, K. Akimoto, and H. Sugiyama, e-J. Surf. Sci. Nanotechnol. **7**, 533 (2009).

[14] I. Barke, F. Zheng, S. Bockenhauer, K. Sell, V. v. Oeynhausen, K. H. Meiwes-Broer, S. C. Erwin, and F. J. Himpsel, Phys. Rev. B **79**, 155301 (2009).

[15] M. Krawiec, Phys. Rev. B **81**, 115436 (2010).

[16] M. Takahasi, S. Nakatani, Y. Ito, T. Takahashi, X. Zhang, and M. Ando, Surf. Sci. **357-358**, 78 (1996).

[17] W. Voegeli, T. Takayama, K. Kubo, M. Abe, Y. Iwasawa, T. Shirasawa, T. Takahashi, K. Akimoto, H. Sugiyama, H. Tajiri, and O. Sakata, e-J. Surf. Sci. Nanotechnol. **6**, 281 (2008).

[18] In the determination of the gold coverage in Refs. 13 and 17 a coverage of 0.4 ML was assumed for the Si(111)-Au-5×2 surface. With a coverage of 0.6 ML for the Si(111)-Au-5×2 surface (Ref. 14) the coverage for the Si(553)-Au surface is close to 0.5 ML.

[19] E. Vlieg, J. Appl. Crystallogr. **30**, 532 (1997).

[20] I. K. Robinson, in *Handbook on Synchrotron Radiation*, edited by G. L. Brown and D. E. Moncton (Elsevier, Amsterdam, 1991), Vol. 3, Chap. 7, pp. 221–266.

[21] See supplementary material at http://link.aps.org/supplemental/10.1103/PhysRevB.82.075426 for a crystallographic information file with fitted atomic coordinates and experimental x-ray intensities.

[22] M. Jałochowski, M. Stróżak, and R. Zdyb, Surf. Sci. **375**, 203 (1997).

[23] P. Segovia, D. Purdie, M. Hengsberger, and Y. Baer, Nature (London) **402**, 504 (1999).

[24] I. K. Robinson, P. A. Bennett, and F. J. Himpsel, Phys. Rev. Lett. **88**, 096104 (2002).

[25] B. Warren, *X-Ray Diffraction* (Addison-Wesley, Reading, 1969).

[26] G. H. Stout and L. H. Jensen, *X-Ray Structure Determination: A Practical Guide* (Wiley, New York, 1989).

[27] T. Takahashi, K. Sumitani, and S. Kusano, Surf. Sci. **493**, 36 (2001).

[28] D. K. Saldin, R. J. Harder, V. L. Shneerson, and W. Moritz, J. Phys.: Condens. Matter **13**, 10689 (2001).

[29] D. K. Saldin, R. Harder, H. Vogler, W. Moritz, and I. K. Robinson, Comput. Phys. Commun. **137**, 12 (2001).

[30] D. K. Saldin and V. L. Shneerson, J. Phys.: Condens. Matter **20**, 304208 (2008).

[31] S. C. Erwin and H. H. Weitering, Phys. Rev. Lett. **81**, 2296 (1998).

[32] S. C. Erwin, I. Barke, and F. J. Himpsel, Phys. Rev. B **80**, 155409 (2009).

[33] Extracted from Fig. 3 of Ref. 15.

[34] M. Krawiec, Appl. Surf. Sci. **254**, 4318 (2008).

[35] S. Riikonen and D. Sánchez-Portal, Phys. Rev. B **71**, 235423 (2005).

[36] F. Bechstedt, *Principles of Surface Physics* (Springer, Berlin, 2003).